

Geospatial Monitoring of Urban Dynamics and Urbanization Impacts on Urban Green Landscape in Megacity Beijing Using the National Polar-orbiting Partnership Visible Infrared Imaging Radiometer Suite (NPP-VIIRS) Nighttime Light Data and Landsat Imagery (1999–2021)

Yanan Liu,^{1,2*} MengXue Xu,^{1,2} Renjie Li,^{1,2} Ai Zhang,^{1,2} and Peng Gao^{1,2}

¹School of Geomatics and Urban Spatial Informatics, Beijing University of Civil Engineering and Architecture, No. 1 Zhanlanguan Road, Xicheng District, Beijing 100044, China

²Engineering Research Center of Representative Building and Architectural Heritage Database, No. 15 Yongyuan Road, Daxing District, Beijing 102616, China

(Received August 9, 2024; accepted March 31, 2025)

Keywords: urbanization, urban green, urban expansion, spatial comparison method, landscape pattern

Urbanization can lead to social and economic progress, but it also inevitably poses a threat to the urban environment and ecological systems, especially in a fast-growing metropolis. Quantifying spatiotemporal patterns of urban expansion and its impact can help optimize land use patterns and promote sustainable urban development. In this study, we propose a novel methodological framework that (1) incorporates a spatial statistics approach for extracting built-up areas and a comprehensive evaluation method for assessing landscape changes, from overall trends to detailed internal dynamics, and (2) aims to quantify urban dynamics and investigate their impacts on urban green spaces. The time-series National Polar-orbiting Partnership Visible Infrared Imaging Radiometer Suites (NPP-VIIRS) imagery and statistical data including geographic information system (GIS)-based analysis were used to calculate overall changes in urban land expansion speed and movement direction, respectively. The spatiotemporal characteristics of urban green landscape patterns (i.e., landscape-level and class-level metrics) were monitored with time-series Landsat images. The results indicate that urban areas have experienced rapid expansion, and the built-up area increased by 1008.75 km² in the past 20 years. The urban expansion indices - including the expansion rate, intensity, and changes in urban migration center of gravity - reveal a distinct spatial structure of urban growth. This pattern was marked by both leapfrog development and the contiguous expansion of existing urban areas. Between 1999 and 2021, the gravity center of urban land consistently shifted in various directions. The area of built-up land decreased by -1.86% from 2014 to 2021, resulting in negative growth. Urban expansion has significantly altered the landscape pattern of urban green spaces, leading to the increased degree of fragmentation of built-up lands and a reduction in landscape diversity. Overall, geospatial monitoring is crucial in understanding how urban

*Corresponding author: e-mail: liuyanan@bucea.edu.cn
<https://doi.org/10.18494/SAM5299>

expansion affects urban green spaces and can provide more balanced and informed decision-making in urban growth.

1. Introduction

Rapid urbanization is coupled with environmental issues, particularly problems affecting the vegetation ecosystem.^(1–3) The expansion of the urban scale can improve urban capacity and promote economic development. However, the expansion of urban construction land will break the original ecological landscape pattern and even lead to the fragmentation of the urban green landscape and a reduction in biodiversity. Therefore, it is vital to monitor and analyze the evolution of urban construction land and urban green landscape patterns for the urban planning management and ecological environment protection of megacities.

The rapid development of remote-sensing technology has been widely used in studying urban expansion and landscape ecology, significantly advancing urban expansion and landscape pattern analysis. Satellite-based artificial nighttime light (*NTL*) observations provide a unique proxy measure for revealing urbanization and regional development, with the advantage of large-scale and small storage, which can effectively reflect the intensity of human activities.^(4–6) The widely used National Polar-orbiting Partnership Visible Infrared Imaging Radiometer Suites (NPP-VIIRS) dataset has a spatial resolution of 500 meters and can detect light radiation across a broad spectral range from 0.3 to 14 μm .^(2,7,8) In addition, imagery such as Landsat is widely used in the dynamic change analysis of landscape patterns.^(9,10)

Urban area mapping and urbanization estimation methods can be summarized into three categories on the basis of statistical data: threshold-based methods, and supervised classification, and spatial comparison methods.^(2,11,12) In threshold-based methods, the threshold can be determined on the basis of experience,⁽¹³⁾ mutation detection,⁽¹⁴⁾ segmentation,⁽¹⁵⁾ and spatial comparison based on auxiliary data.⁽¹⁶⁾ Supervised classification methods map urban areas using traditional classification algorithms and machine learning methods.^(17,18) The basic idea of the spatial comparison method based on statistical data is to use relevant auxiliary and *NTL* remote sensing data to determine the optimal threshold for urban extraction.⁽¹⁶⁾ In China, the Ministry of Land and Resources publishes annual urban land statistics. However, statistical data that rely on administrative units lack spatial information, making it difficult to meet the requirements of large-scale research on the spatial patterns of Chinese cities. Therefore, a methodological framework is needed to map urban areas by combining statistical data and remote sensing imagery.

Studying the correlation between urban expansion and landscape patterns is an effective way of exploring the ecological effects of urban expansion.^(19,20) Tagil, Gormus, and Cengiz⁽²¹⁾ explored the relationship between urban expansion, landscape patterns, and ecological processes in Denizli, Turkey, using Landsat satellite imagery from 1987 to 2013, which revealed changes in habitat and presented the landscape characteristics based on the assessment of landscape pattern indicators. Su *et al.*⁽²²⁾ measured the impact of urban sprawl on natural landscape patterns using insulation degree metrics in the western Taihu Lake Watershed, China, and concluded that the most critical natural landscape elements for maintaining overall connectivity could be easily identified using these metrics. Monitoring and analyzing the change in vegetation landscape

pattern in the context of urbanization are instrumental in determining the relationship between landscape pattern change and human social activities, and quantifying the impact intensity and direction of the factors that lead to the change. Karim *et al.*⁽²³⁾ investigated urban expansion patterns in Lahore between 1998 and 2023 with Landsat imagery. Their analysis revealed rapid and unplanned urban sprawl, particularly along major transportation corridors. Messaoud *et al.*⁽²⁴⁾ investigated changes in land use and landscape patterns in Tunis between 2000 and 2020, and explored the relationship between urban expansion and the decline of green infrastructure.

In this study, we investigated the evolution of urban expansion and its impact on landscape patterns, particularly urban green landscape patterns, using NPP/VIIRS, Landsat imagery, and statistical yearbook data from 1999 to 2021 in Beijing, the capital of China. The main purposes of this study were to (a) reveal the spatial and temporal characteristics of megacity expansion, (b) explore the spatiotemporal evolution of urban green landscape patterns, and (c) analyze the relationship between urbanization and the evolution of urban green landscape patterns.

2. Materials and Methods

2.1 Study site

The study site is located in Beijing and covers an area of 16410 km², as illustrated in Fig. 1, which is located in the northern part of North China (39°28′–41°05′ N, 115°25′–117°30′ E). The terrain is elevated in the northwest and decreases in elevation towards the southeast, with an

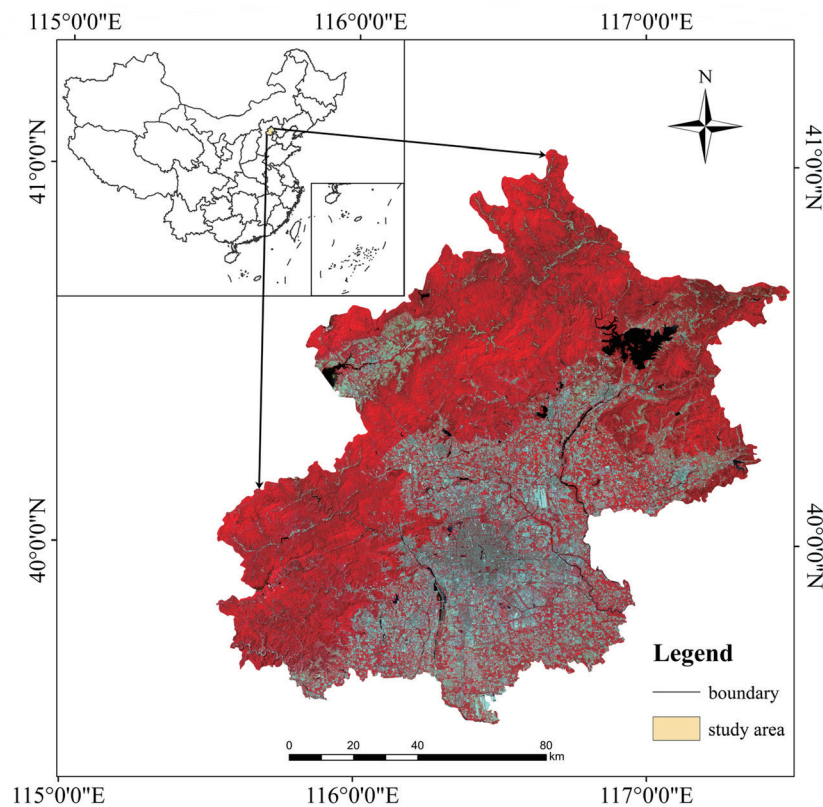


Fig. 1. (Color online) Overview of study area.

average altitude of 43.5 m. It is a political, cultural, technological, and educational center in China, with an urbanization rate of 87.5%, classifying it as a megacity. The west, north, and northeast of Beijing are surrounded by mountains, and the vegetation cover is dominated by natural forests. The central part is an open plain to the southeast and is a well-developed city. The vegetation cover is mostly artificial, and farmlands dominate the southeastern part. The vegetation is primarily composed of warm-temperate deciduous broadleaf forests and temperate coniferous forests.

2.2 Data and preprocessing

The obtained datasets are NPP-VIIRS-like *NTL* data, Landsat series images, and the data from the Beijing statistics yearbook, as shown in Table 1.

The “NPP-VIIRS-like” data is a global night light dataset with a resolution of 500 m.⁽²⁵⁾ It is based on the correction of the cross-sensor (DMSP-OLS and NPP-VIIRS) *NTL* data using an autoencoder, making it possible to use the night light data across long time series. We preprocessed it by resampling, defining projections, and clipping, and used it to extract built-up areas and conduct a study of urban expansion.

The Landsat satellites are a series of Earth observation satellite systems launched by the United States since 1972 for detecting earth resources and the environment. We obtained Landsat satellite images from the Chinese Academy of Sciences Geospatial Data Cloud (<http://www.gscloud.cn>). These images were obtained during the period of lush vegetation growth from 1999 to 2021 at times when there was minimal cloud cover. Each image was obtained using systematic radiometric correction, geometric correction, and digital elevation model (DEM) terrain correction before being downloaded. Therefore, in this study, we only performed the preprocessing of radiometric calibration, atmospheric correction based on the FLASH atmospheric correction model, mosaicking, and cropping.

The Beijing Statistical Yearbook (<http://tjj.beijing.gov.cn>) is a book compiled by the Beijing Municipal Bureau of Statistics that reflects the development and changing trends of Beijing’s major economic and social indicators from multiple fields and industries. It covers the most comprehensive and authoritative comprehensive statistical data on Beijing’s development. We obtained the built-up area of Beijing from the Beijing Statistical Yearbook and used the statistical data comparison method of He *et al.*⁽¹²⁾ to determine the light threshold that needs to be extracted from night light remote sensing data and to obtain the geographical distribution of the built-up area. We utilized Landsat imagery from 1999 to 2021 and NPP-VIIRS data from 2000 to 2021 for our analysis. Although the two datasets cover slightly different periods, this discrepancy does not affect the results, as the focus is on built-up areas, which remained unchanged over the two years according to the statistical yearbook.

Table 1
Description of the remote sensing dataset used.

Data type	Acquisition date	Resolution (m)
Nighttime Light Imagery	2000/2003/2009/2014/2020	500 (Resampled)
Landsat-7 ETM Images	1999-8-2; 2003-7-28; 2009-8-13	30
Landsat-8 OLI Images	2014-8-19; 2021-8-6	

2.3 Methods

The proposed approach was employed to examine the spatiotemporal evolution of urban expansion, and its subsequent influence on urban green landscape patterns within Beijing from 1999 to 2021 is illustrated in Fig. 2. By leveraging long-term satellite imagery (NPP-VIIRS and Landsat), we extracted urban sprawl data and computed expansion indices. In addition, landscape metrics were applied to comprehensively assess both overarching trends and intricate internal alterations within urban green landscapes, affording insights into the migratory patterns of urban centers and the repercussions of urbanization on urban green space configurations.

2.3.1 Extraction of urban expansion indices

The characteristics of urban expansion were analyzed from both temporal and spatial perspectives. The indices for urban expansion are the average annual expansion rate, average

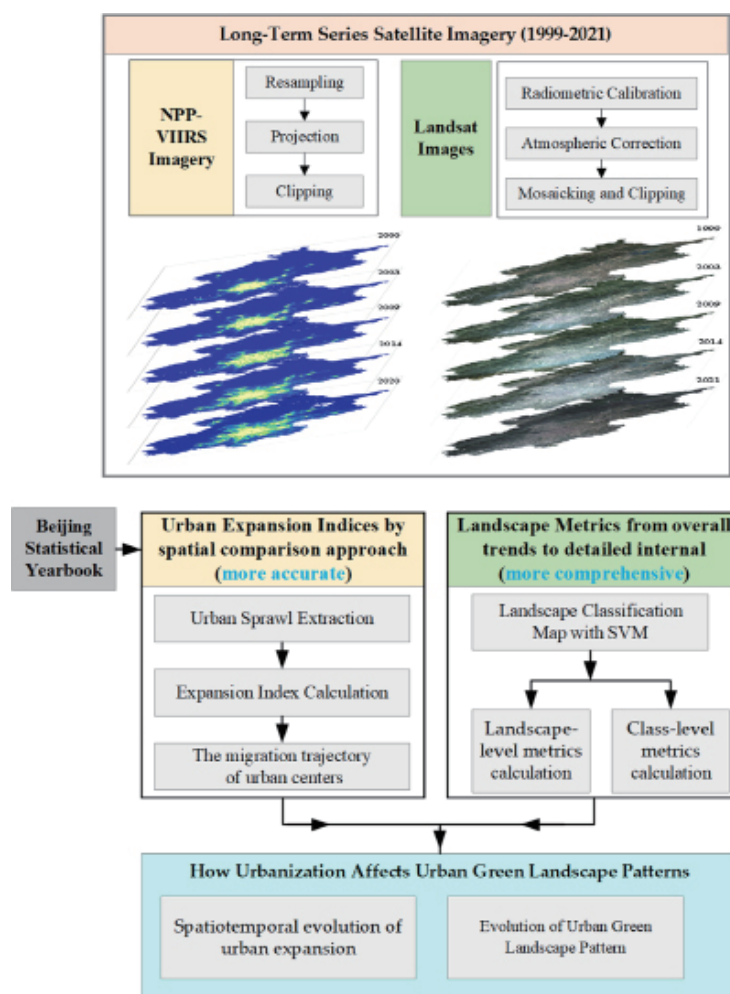


Fig. 2. (Color online) Pipeline of the proposed approach in the research.

annual expansion intensity (*UEI*), and the center of gravity of urban migration changes, which are derived from the built-up lands in Beijing. To accurately capture built-up areas, a new spatial comparison approach was proposed and applied to the time-series NPP-VIIRS imagery.⁽²⁶⁾ NPP-VIIRS remote sensing images, which reflect the frequency of human activities in a region, provide essential information for understanding and studying urban development. Time series data on changes in built-up areas can accurately capture shifts in urbanization levels and urban development dynamics, allowing for the study of urban growth patterns and the analysis of the driving factors behind urban development. Compared with visible light remote sensing data, *NTL* remote sensing data not only reflect the spatial extent of urbanization but also serve as a direct indicator of human activities, showing a strong correlation with socio-economic variables. Therefore, we first merged the pixels with the same values and calculated their areas. We then established the initial threshold by comparing the calculated built-up areas with the reference area from the officially published *NTL* data. This process was repeated until the threshold closest to the actual value in the *NTL* data was identified, establishing it as the critical value for urban built-up area extraction. These steps are repeated until the final threshold, which is closest to the true value in the *NTL* data, is determined. This threshold allows for the accurate extraction of urban built-up areas.

The average annual expansion rate (V_t) reflects the change in urban built-up area expansion over time and is commonly used to indicate the speed of spatial expansion across different periods, as demonstrated in Ref. 27. The formula used is

$$V_t = \left(T \sqrt{\frac{S_b}{S_a}} - 1 \right) * 100\%, \quad (1)$$

where S_a is the urban built-up area in the early stage, S_b is the urban built-up area in the late stage, and T is the time interval.

The *UEI* index can measure the expansion status of countries or cities at different stages vertically and facilitate the comparison of expansion intensity at the same stage horizontally, as shown in Refs. 28 and 29. *UEI* refers to the ratio of the expanded built-up area over a certain period to the total built-up area.⁽²⁷⁾ The formula is

$$UEI = \frac{S_b - S_a}{TLA} * \frac{1}{T} * 100\%, \quad (2)$$

where S_a and S_b are the early and current urban built-up areas, and T and TLA are the time interval and the total area, respectively.

The brightness values of *NTLs* in built-up areas reflect the level of development within a city. By using the grayscale values of *NTL* imagery pixels in built-up areas as weights, we can calculate the city's center of gravity and plot the trajectory of its shift. This allows us to assess trends in regional economic and population changes and analyze their causes. The coordinates for the center of gravity in built-up areas are calculated as⁽²⁸⁾

$$\begin{aligned}\bar{X} &= \frac{\sum_{i=1}^n M_i \cdot X_i}{\sum_{i=1}^n M_i}, \\ \bar{Y} &= \frac{\sum_{i=1}^n M_i \cdot Y_i}{\sum_{i=1}^n M_i}.\end{aligned}\tag{3}$$

2.3.2 Landscape metrics

With the acceleration of urbanization, urban space constantly expands, dramatically changing the landscape patterns of urban land use. To analyze the evolution of landscape patterns, the main landscape types were determined to be forest, grassland, farmland, construction land, bare land, water, and artificial vegetation on the basis of the actual distribution at the study site. The landscape classification map was obtained by the support vector (*SVM*) method for each time interval.

To analyze the characteristics of urban green landscape patterns in the context of urban expansion, four class- and landscape-level metrics were selected on the basis of a grid map of landscape types in different years ($30 \times 30 \text{ m}^2$) in this study. At the landscape level, Shannon's diversity index (*SHDI*), patch density (*PD-L*), and edge density (*ED*) were used to characterize the overall diversity, fragmentation, and complexity of the landscape. The *PD-Cs* were selected at the class level. Spatiotemporal changes in landscape patterns were analyzed using the established indicators. Specific descriptions of the landscape metrics are presented in Table 2.

3. Results

3.1 Characteristics of urban expansion from 1999 to 2021

3.1.1 Spatiotemporal evolution of urban expansion

Exploring the spatial characteristics of a dynamic urban expansion is important for regional planning and development. In this study, built-up areas were extracted for the years 1999, 2003, 2009, 2014, and 2021 using NPP-VIIRS images. The spatial distribution and area statistics of built-up land for these years are presented in Fig. 3. In addition, the patterns of urban expansion were analyzed.

The degree of spatial expansion is a key factor in measuring the level of urbanization. Therefore, we obtained the built-up area and created five maps of built-up areas at different times (1999, 2003, 2009, 2014, and 2021), as presented in Fig. 3. The city has been undergoing urban expansion over the past two decades. The built-up area was expanded from 494 km^2 in 1999 to 1502.75 km^2 in 2021, while the areas in 2003, 2009, and 2014 were 648.25 , 1321 , and 1348.25 km^2 , respectively.

Moreover, the urban expansion (Fig. 4) was obtained by overlaying the built-up areas from 1999 to 2021. Built-up areas exhibited a marginal expansion pattern from 1999 to 2003, extending outward from the city center in all directions. The well-developed infrastructure in

Table 2
Multiple landscape metrics were used in this study.

Level	Metric (Abbreviation)	Range	Description
Landscape	Patch Density (<i>PD-L</i> , number/hm ²)	(0, +∞)	The total number of patches in the landscape is divided by the total landscape area.
	Edge Density (<i>ED</i> , m/ha)	[0, +∞)	The sum of the lengths of all edge segments in the landscape is divided by the total landscape area.
	Shannon's Diversity Index (<i>SHDI</i>)	[0, +∞)	The negative sum, across all patch types, of the proportional abundance of each patch type is multiplied by the logarithm of that proportion.
Class	Patch Density (<i>PD-C</i> , number/hm ²)	(0, +∞)	The number of patches of the corresponding patch type is divided by the total landscape area.

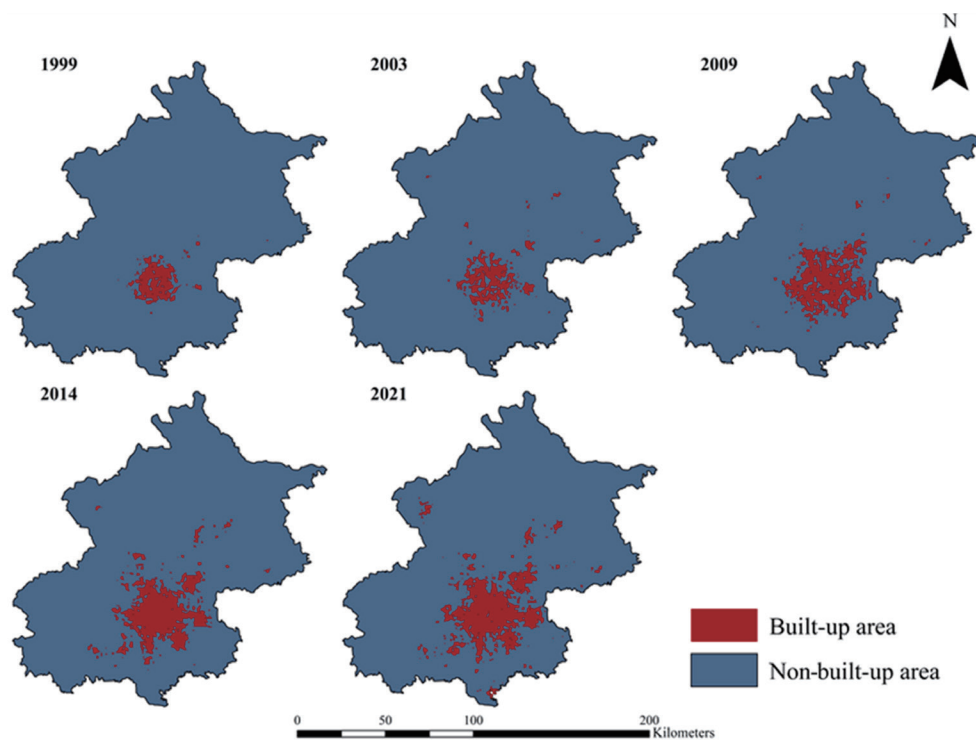


Fig. 3. (Color online) Spatial distribution of urban built-up areas from 1999 to 2021.

the central urban area facilitated the growth and development of surrounding areas, leading to the conversion of other land types into construction land. From 2003 to 2014, urban sprawl was characterized by marginal expansion, with an emphasis on infill development. This means that the original old urban areas were transformed and replaced to improve the strength of the original construction land and enrich urban functions. During the period from 2014 to 2021, urban sprawl continued to be primarily driven by marginal expansion, although it was accompanied by rapid growth, and the layout of the increased built-up land is relatively scattered.

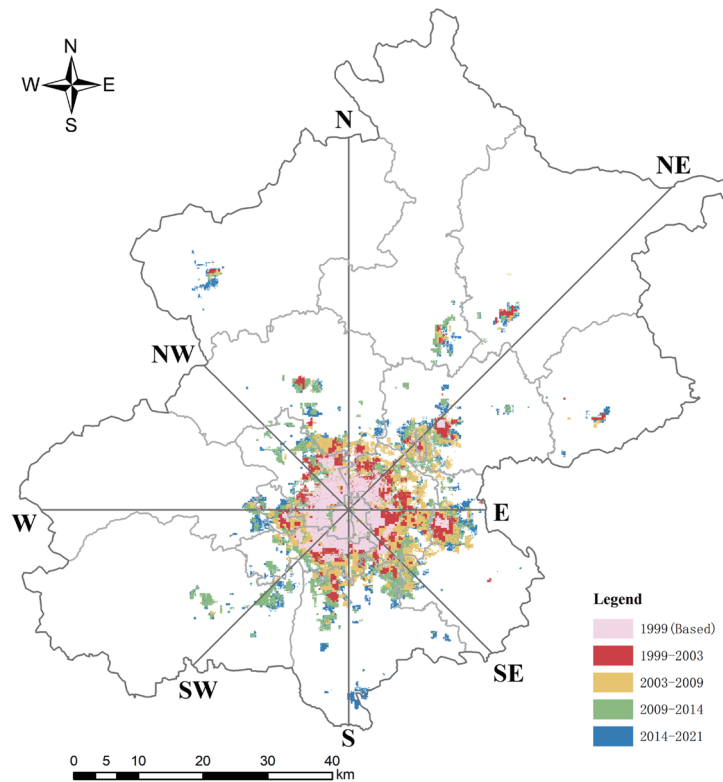


Fig. 4. (Color online) Urban expansion from 1999 to 2022.

3.1.2 Scale characteristics of built-up area expansion

The spatial expansion intensity, the spatial expansion speed of urban built-up areas, and the expansion center of gravity are important indicators for measuring the morphological expansion of urban built-up areas.

Figure 5 reveals that UEI shows distinct differences in eight directions across these periods, similar to the conclusion in the previous study.⁽²⁹⁾ The UEI value in the east was largest from 1999 to 2003 and from 2003 to 2009, indicating that the UEI mainly occurred in this direction before 2009. In addition, the UEI value in the south was high from 1999 to 2003, and the UEI values in the south and southeast were high from 2003 to 2009. This illustrates that the city expanded primarily to the east, south, and southwest between 1999 and 2009. The intensity of urban expansion gradually decreased after 2009, but the urban area expansion occurred in all directions from 2009 to 2014, with notable growth in the southeast and southwest regions. From 2014 to 2021, UEI values showed negative growth in most directions, with the southwest experiencing the lowest UEI value and the south the highest. This indicates a reduction in built-up land across most areas of Beijing, consistent with Beijing's urban planning policy aimed at decreasing construction land and increasing ecological land use.

As shown in Fig. 6, V_t is different for the eight directions in the four time periods from 1999 to 2021. Overall, the V_t of the urban areas first increased and then gradually decreased during this period. This illustrates that Beijing was in a stage of rapid urban expansion from 1999 to

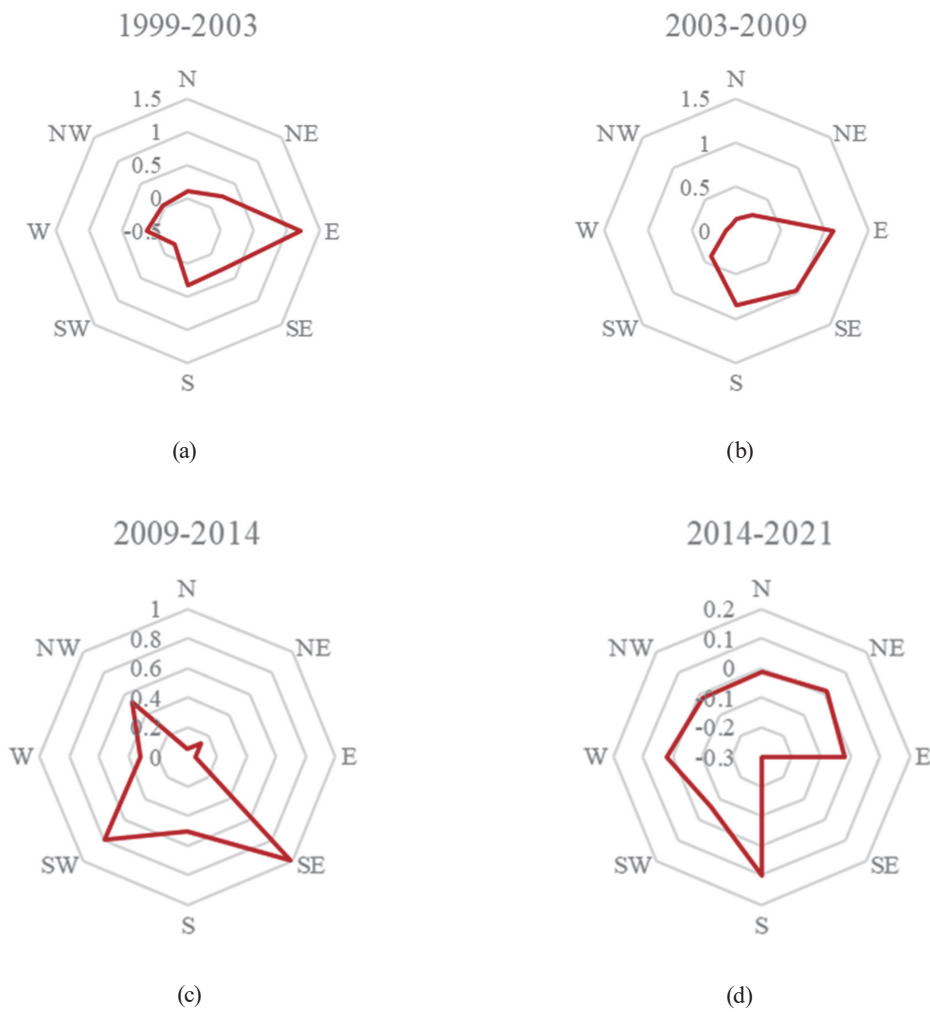


Fig. 5. (Color online) Urban *UEI* for eight directions across four time periods.

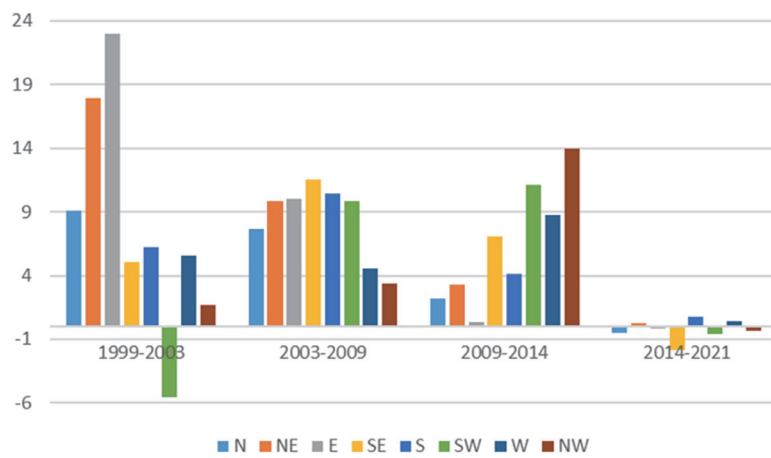


Fig. 6. (Color online) Urban expansion rate (V) for eight directions.

2009. V_t declined gradually from 2009 to 2014, although the urban area was still in the expansion stage. The V_t in most directions was negative from 2014 to 2021, demonstrating that the built-up land area decreased during this period. The results are consistent with the Urban Master Plan and the 3rd National Land Resource Survey,^(30,31) both of which aim to reduce the built-up land area, with the target of decreasing it to 2860 km² by 2021. The V_t values were between -5.55 and 23.00% from 1999 to 2003, and the largest V_t values were in the east and northeast, which were 23.00 and 17.96%, respectively. The V_t values were the lowest in the southwest and northwest directions, and there was negative urban growth in the southwest direction. The V_t values ranged from 3.34 to 11.51% between 2003 and 2009. V_t was similar in most directions, and the V_t values were low in the south and northwest. From 2009 to 2014, urban expansion rates were high in the northwest and southwest, with values of 13.93 and 11.14%, respectively. The urban expansion rate in the east was the lowest, with a value of 0.31%. The V_t values were between -1.86 and 0.72% from 2014 to 2021. The urban area expanded slightly in the east, west, and northwest, and the area of built-up land in the other directions decreased.

Exploring the migration trajectory of a city's center of gravity is significant for the strategic planning of urban development. Figure 7 shows the migration trajectory of the city's center of gravity. The city's center of gravity moved to the northeast, and the movement distance was the largest from 1999 to 2003. The city's center of gravity moved southwest from 2003 to 2009. This illustrates that the development of Beijing moved mainly towards the east from 1999 to 2009. The city's center of gravity moved to the southwest from 2009 to 2014, before moving to the northeast after 2014. Overall, the center of gravity of the city showed negligible change in position.

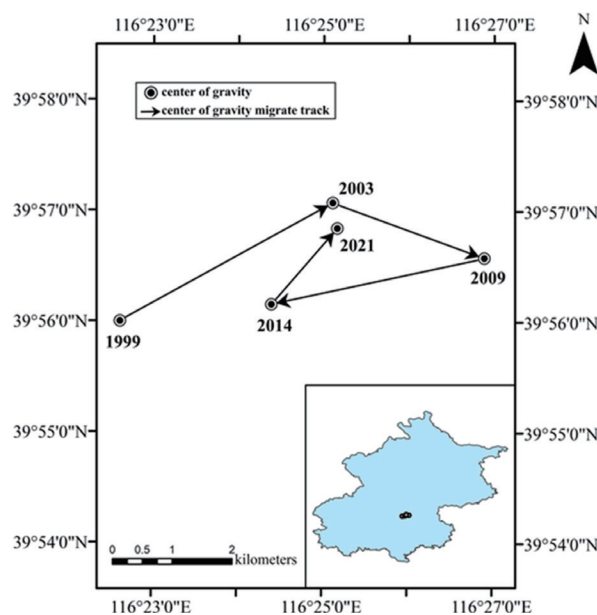


Fig. 7. (Color online) Spatiotemporal migration trajectory of urban areas from 1999 to 2021.

3.2 Evolution of urban green landscape pattern in the context of urban expansion

3.2.1 Extraction of urban green landscapes

Urban green landscapes, including artificial planting vegetation, forest, grassland, farmland, construction land, bare land, and water, were extracted from the Landsat imagery over multiple time intervals by the *SVM* method. The details for each time interval obtained by the *SVM* method are shown in Fig. 8. The overall accuracy was higher than 90%, the kappa coefficient was higher than 0.90, and the final urban green landscape map is illustrated in Fig. 9.

3.2.2 Dynamics of urban green landscape pattern

Exploring the characteristics of the urban green landscape evolution is of considerable significance for urban planning and development. In this study, the *PD-C* index at the class level for four different vegetation types in 1999, 2003, 2009, 2014, and 2021 was calculated, and the *ED*, *PD-L*, and *SHDI* values of the landscape-level index were calculated for the five periods, as illustrated in Fig. 10.

The *PD-C* value at the class level reflects the fragmentation of different landscape types. This can be observed in Fig. 10, where the *PD-C* of the artificial planting urban green landscape experienced a decline first and was the lowest in 2009 at 5.50 number/hm², then increased slowly and remained relatively high. This indicates that the degree of fragmentation of artificial planting in the urban green landscape decreased before 2009 and then gradually increased. The distribution of forests had the characteristics of aggregation; therefore, the *PD-C* value has changed negligibly over the past 20 years and was the lowest in the urban green landscape types.

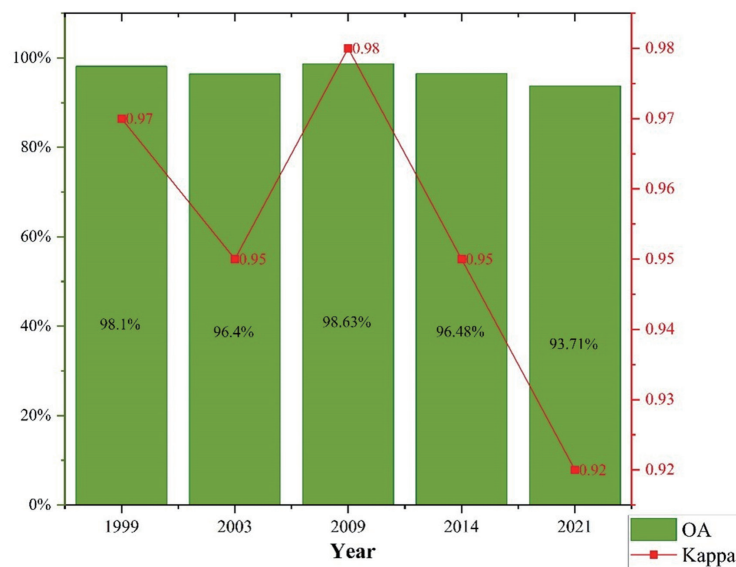


Fig. 8. (Color online) Detailed precision for *SVM* classification.

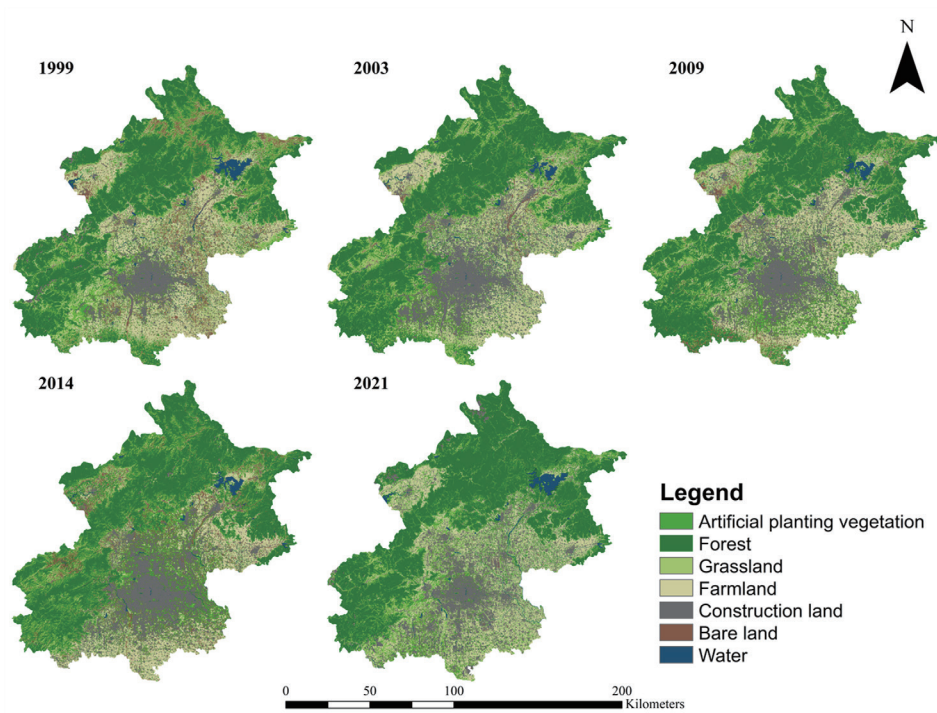


Fig. 9. (Color online) Spatial distribution map of landscape types based on SVM from 1999 to 2021.

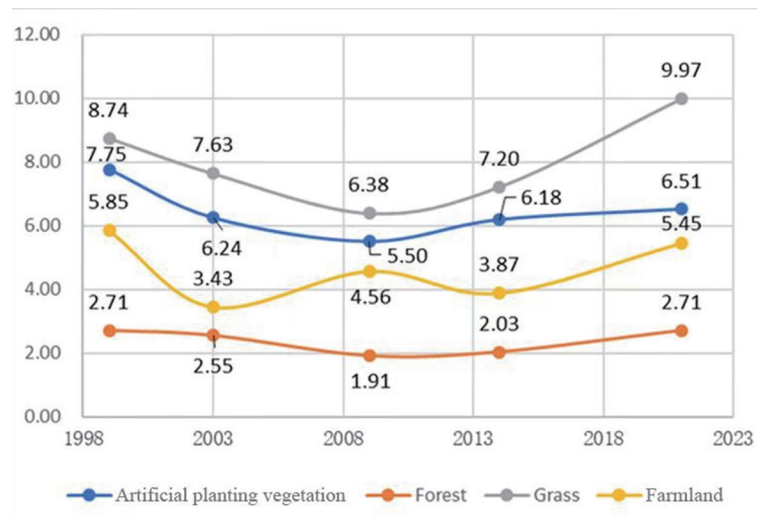


Fig. 10. (Color online) PD-C value for different vegetation types from 1999 to 2021.

The *PD-C* value of grassland was the highest among all urban green landscapes, ranging from 6.38 to 9.97 number/hm². This indicates that grass was the most fragmented. The *PD-C* value first decreased and then increased from 1999 to 2021. The *PD-C* value of grassland was the lowest in 2003 (6.38 number/hm²) and the highest in 2021 (9.97 number/hm²). The *PD-C* value

of farmland fluctuated considerably, but the degree of fragmentation was always below that of artificially planted vegetation and grassland. During urban development, the change characteristics of the *PD-C* value for artificially planted vegetation, forest, and grassland with ecological service functions were similar. They all experienced a process of having first decreased, reaching their lowest levels in 2003, before increasing.

Figure 11 shows the *ED*, *PD-L*, and *SHDI* values at the landscape level between 1999 and 2021. Overall, these indices at the landscape level showed a decreasing trend first, then stabilizing for a period before slowly increasing. *PD-L* was largest in 1999, with a value of 34.06 number/hm², and then dropped sharply, showing a slowly increasing trend from 2009 to 2021. This suggests that the landscape exhibited the highest degree of fragmentation in 1999, and over the 20 years, this highly fragmented landscape pattern in Beijing has improved. However, there still exists a relatively high degree of fragmentation. The *ED* value in Beijing was relatively high, initially decreasing before increasing. It was the highest in 1999 at 122.82 m/ha and the lowest in 2003 at 96.29 m/ha. Despite the city's development, the *ED* value in 2021 remains high at 108.1 m/ha. This illustrates that the landscape boundary was highly segmented, the shape of the landscape patch was complex, the interaction and effect of the patch edges were evident, and the edge effect was strongly pronounced. The high edge and patch densities suggest a high degree of landscape fragmentation. In a landscape system, the richer the land use, the higher the degree of fragmentation, the greater the information content of its uncertainty, and the higher the calculated *SHDI* value.^(32,33) The *SHDI* values for Beijing ranged between 1.51 and 1.65. On the one hand, this signifies that Beijing had a high degree of landscape diversity and rich landscape types. However, a high *SHDI* value was more likely to be affected by a high degree of landscape fragmentation.

3.2.3 Spatiotemporal dynamic characteristics of urban green landscape pattern in built-up area

With the advancement of urban expansion, human activities have altered urban green landscape patterns. To investigate the impact of urbanization on urban green landscapes, we

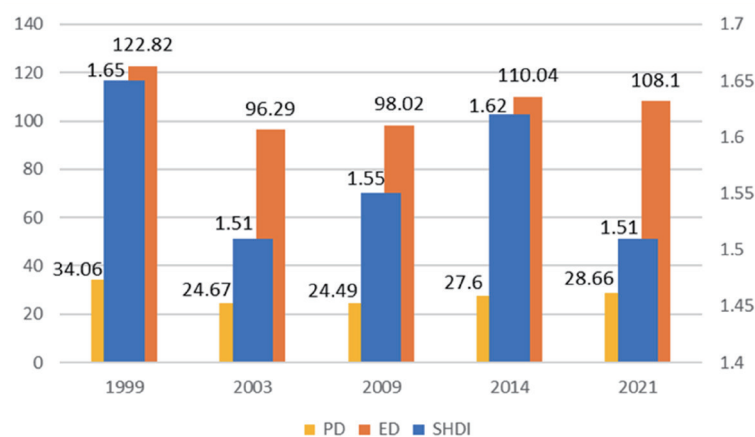


Fig. 11. (Color online) *ED*, *PD-L*, and *SHDI* values of the landscape-level index for different years.

conducted statistical computations and spatial analysis for *ED*, *PD-L*, *SHDI*, and *PD-C* at the class level of artificially planting urban green landscapes from 1999 to 2021.

Figure 12 shows the *PD-L*, *ED*, and *SHDI* values at the landscape level and their changes in built-up areas in Beijing from 1999 to 2021. The *PD-L* and *ED* indices showed the same trend of decreasing first and then increasing, and when *PD-L* and *ED* changed significantly, *SHDI* also exhibited a similar trend. From 1999 to 2014, in the urban built-up area of Beijing, the *PD-L* value of the landscape varied between 1.3 and 2.3%; however, in 2021, there was a significant increase, reaching as high as 4.399 number/hm². This indicates that the landscape in the built-up areas of Beijing presented a certain degree of fragmentation and was most significant in 2021. The *ED* values in the built-up areas showed the same trend as the *PD-L* values. From 1999 to 2014, *ED* fluctuated between 5.4587 and 8.4981 m/hm² and reached its highest value in 2021 (13.3417 m/hm²). The change in *ED* shows that the degree of segmentation of landscape boundaries in the built-up areas of Beijing went from low to high, directly reflecting the increasingly fragmented landscape patches. The *SHDI* value of the landscape in the built-up areas of Beijing shows an upward trend, particularly in 2021, when the *SHDI* value reaches 1.0753. This change indicates that there is a certain diversity of landscapes in the built-up areas of Beijing. As the number of landscape patches increased, *SHDI* also increased.

The spatial distribution of *PD-L* values in the built-up areas of Beijing in different years is illustrated in Fig. 13, where the areas with high *PD-L* values were mainly distributed on the edges of the built-up areas. With the city's development, areas with high *PD-L* values appeared at the center. By 2021, most landscapes in the built-up areas had high *PD-L* values, and the landscape patches were more fragmented than in previous years. This shows that while the scope of urban landscape fragmentation expanded, it also gradually affected the central area of the city. Areas with high *PD-L* values in 1999 and 2003 were mainly distributed in the northern

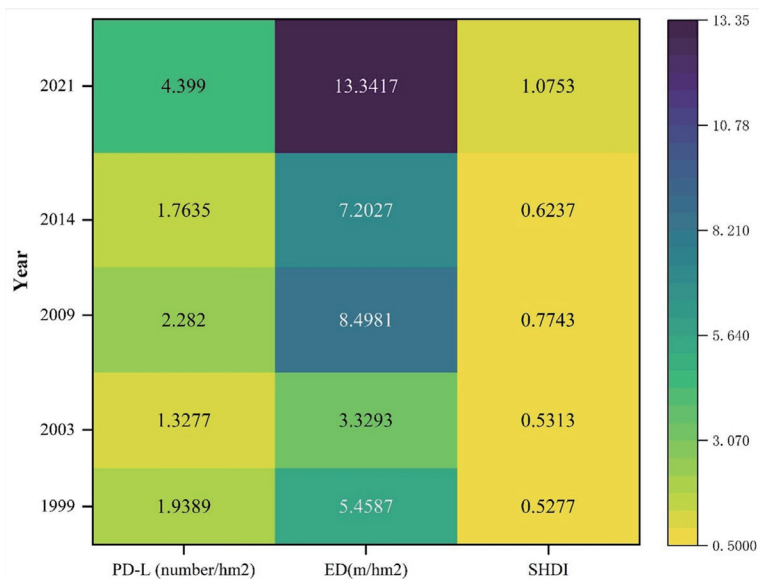


Fig. 12. (Color online) Values of landscape-level indices in different stages.

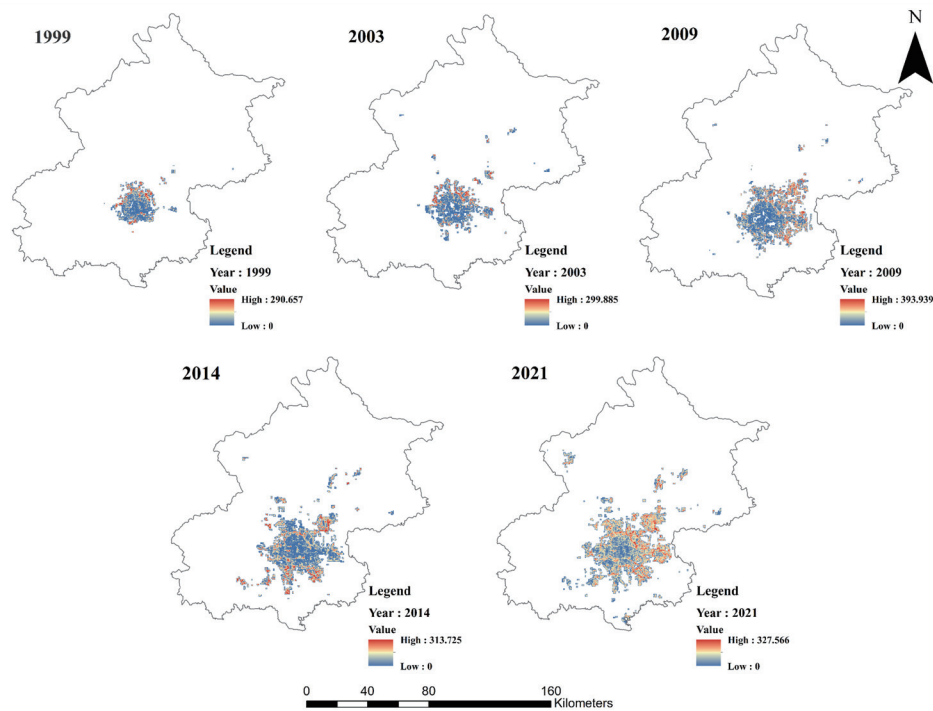


Fig. 13. (Color online) Map of $PD-L$ in different years.

region, whereas from 1999 to 2003, the expansion was mainly from east to north. In 2009, areas with high $PD-L$ values were mainly distributed in the east, whereas the expansion speed of the eastern area was relatively high from 2003 to 2009. Compared with 2009, the western expansion in 2014 was clear, and the $PD-L$ value in the expansion area in 2014 was also high. In 2021, most of the built-up areas exhibited relatively high $PD-L$ values. Although the expansion rate of urban construction land remained zero between 2014 and 2021, the total size of built-up areas was the highest in 2021. This shows that urban sprawl affects landscapes to a certain extent, and as a result, the landscape tends to be more fragmented in these areas.

The spatial distribution of ED values in the built-up areas of Beijing from 1999 to 2021 is mapped in Fig. 14. The ED values around the built-up areas in Beijing were generally higher, whilst those in the central area were lower, suggesting that the landscape patches at the edge of the built-up areas were small, fragmented, and strongly divided, exhibiting a large total length of the landscape edge per unit area. Within built-up areas, the distribution of landscape patches of the same type was consecutive and aggregated, and the total length of landscape edges per unit area was small. The high ED value phenomenon in the built-up area developed from the surrounding area to the city center over time, indicating that in the middle of the built-up area, the integrity and continuity of the landscape patches were gradually broken, and landscape fragmentation intensified. The edge of the built-up area was located in the suburbs, where the impermeable surface transitioned into other landscapes. This region was characterized by complex land types, scattered patches, and varying land types. As a result, the density of landscape edges was high. The interior of the built-up area was dominated by mature,

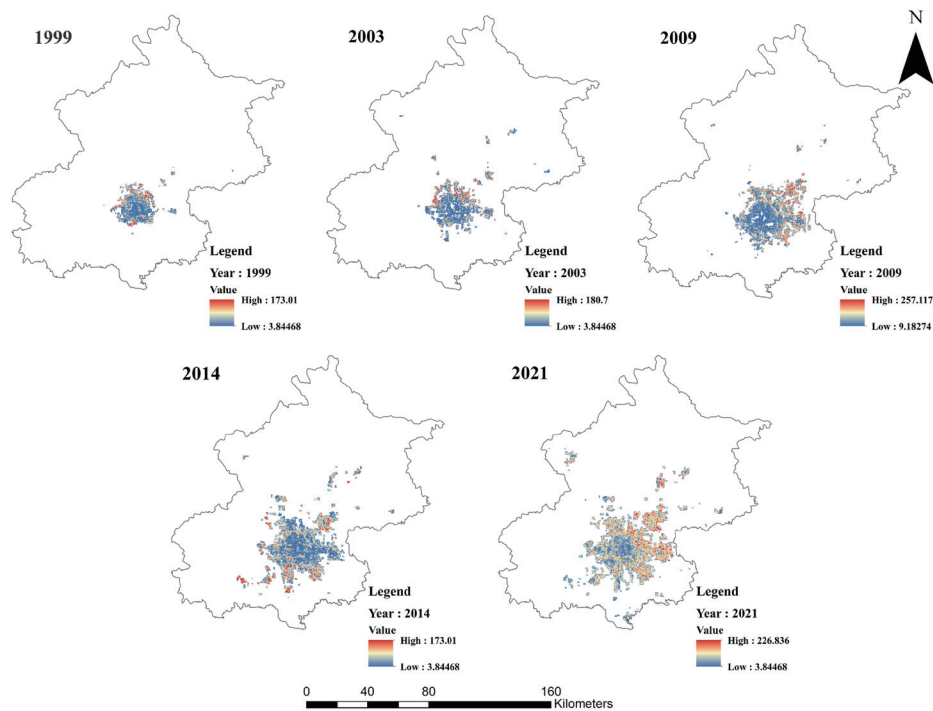


Fig. 14. (Color online) Spatial distribution map of *ED* for different years.

continuous, and densely packed land used for construction, which reduced the degree of crosscutting and overlapping of different landscape patches. Thus, the edge density of the landscape was low. In 1999 and 2003, because the built-up area of Beijing was relatively small and in the early stage of the urban core area, it was dominated by the large-scale and continuous distribution of impermeable surfaces, and there were extensive regions of vegetation and other landscape patches, high *ED* values were concentrated in a small part of the edge of the built-up area. From 2009 to 2021, the built-up area consistently exhibited high *ED* values, reflecting the maturation of the urban core. Concurrently, the number of vegetation patches within the built-up area increased, leading to an expansion of high *ED* zones toward the interior of the urban landscape.

Figure 15 shows that the *SHDI* at the center of the built-up area in Beijing was low, and the areas with high *SHDI* values were mainly distributed at the edges of the original built-up area and recently constructed built-up areas. With the expansion of built-up areas, the distribution area of high *SHDI* values expanded from the edge to the center. In 2021, the built-up areas recorded the highest *SHDI* values, with a notable increase in the central built-up zones, as observed through spatial visualization. The distribution and changes in landscape *SHDI* values in built-up areas indicate that there were more types of landscape found at the edges of built-up areas than in the central areas, and with urban development, the diversity and heterogeneity of landscapes inside built-up areas increased. Urbanization connects construction land, making it the dominant landscape and reducing diversity in urban centers. Moreover, urbanization at the city's edge causes land type changes and fragmentation, increasing landscape diversity in those areas.

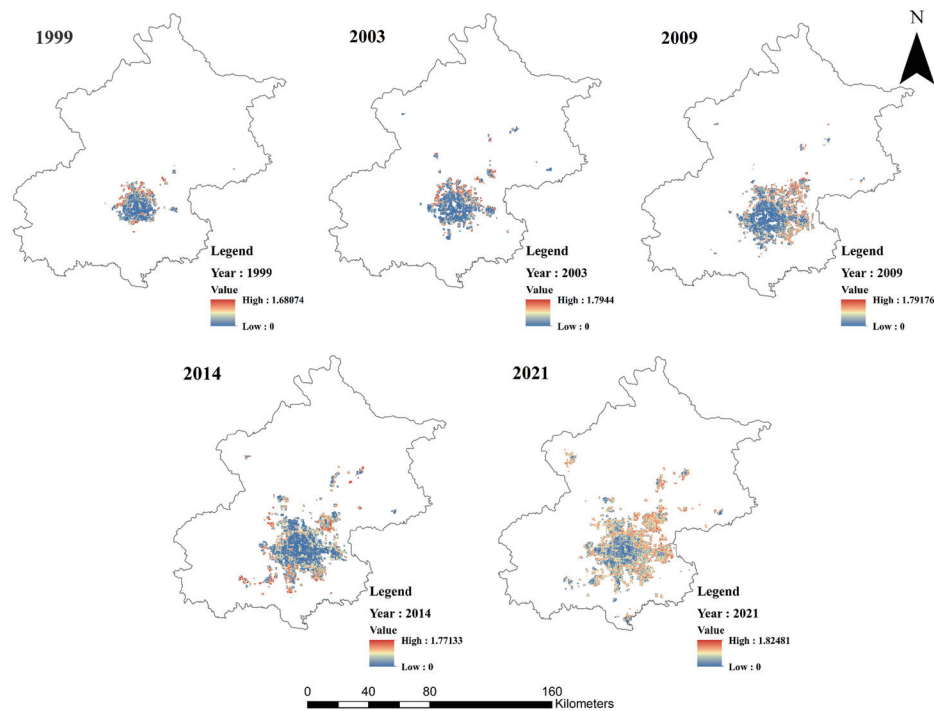


Fig. 15. (Color online) Spatial distribution map of *SHDI* for different years.

With the gradual maturity of urban development, further improvement of urban functions, and further balance of various landscape types, particularly the increase in the proportion of vegetation, the diversity of urban landscapes has increased.

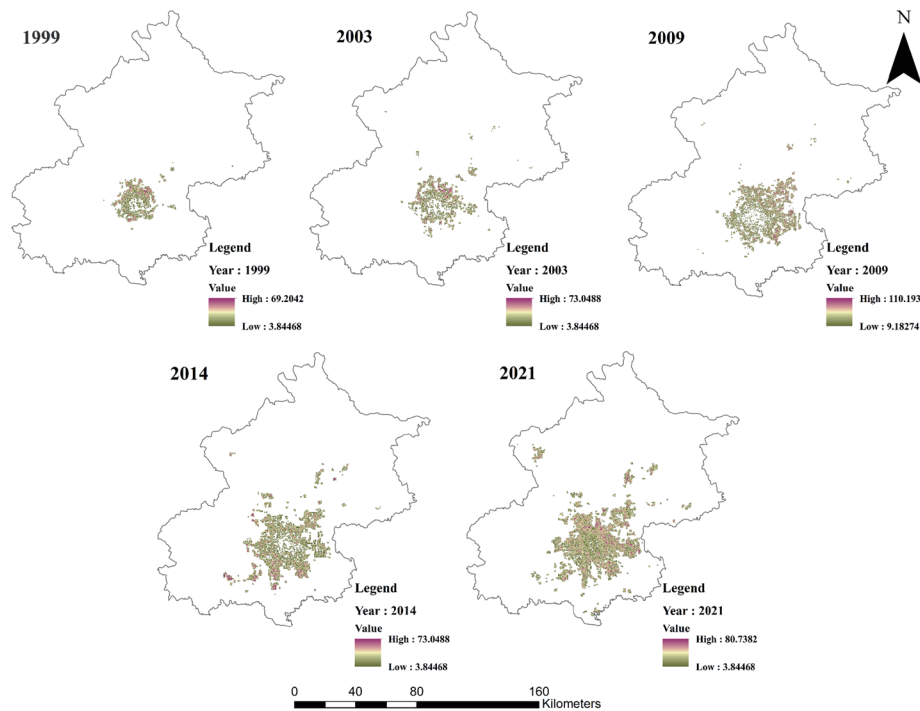
Table 3 shows the areas and *PD-C* values at the class level for artificially planted vegetation in 1999, 2003, 2009, 2014, and 2021. The area of artificially planted vegetation decreased slightly from 1999 to 2003 and then increased substantially from 2003 to 2021, especially from 2003 to 2009. This illustrates that the urban green ecological space was built on a large scale, and the ecological environment improved continuously at the study site. The *PD-C* values for artificially planted vegetation ranged from 0.5432 to 1.2994 during this period. The *PD-C* value showed a downward trend from 1999 to 2003, which may have been due to the reduction in the area for the artificial planting of vegetation. The *PD-C* value of artificially planted vegetation increased significantly from 2003 to 2009, indicating that the number of patches increased with the artificially planted vegetation area, and the degree of landscape fragmentation was higher. These values showed a downward trend in 2009 and 2014. Although the area covered by artificially planted vegetation has increased, the degree of landscape fragmentation has decreased. The *PD-C* value increased from 2014 to 2021, demonstrating that the degree of landscape fragmentation will increase with area.

Figure 16 reveals that the *PD-C* value at the class level for the artificially planted vegetation showed a radial distribution. The value at the center of the city was the smallest and gradually increased towards the edge of the city. This illustrates that artificially planted vegetation has a low degree of fragmentation, good connectivity in downtown areas, and a high degree of

Table 3

PD-C value at class level and areas of artificial planting vegetation in different years.

Year	1999	2003	2009	2014	2021
Area (km ²)	25.8102	22.2399	108.7101	145.9197	148.9284
<i>PD-C</i> (number/hm ²)	0.8761	0.5432	1.1614	0.8505	1.2994

Fig. 16. (Color online) Spatial distribution map of *PD-C* at class level for artificially planted vegetation.

landscape fragmentation at urban fringes. Additionally, the area of artificially planted vegetation in downtown areas will gradually increase from 1999 to 2021, and the degree of fragmentation will also increase. However, the *PD-C* value was lower than that of the urban fringes. The *PD-C* values in the north and northeast were high in 1999 and 2003, indicating that the artificially planted vegetation in this area was highly fragmented during this period. The high *PD-C* value was mainly located in the east, and the area of artificially planted vegetation increased considerably by 2009. This demonstrates that the degree of fragmentation also increases with the number of patches. The *PD-C* value was high in Southwest China in 2014. This may be because the artificial vegetation in this area was newly planted and lacked planning. In addition, the area of artificially planted vegetation in downtown areas increased with a low degree of fragmentation between 2009 and 2014. The area of artificially planted vegetation further increased from 2014 to 2021, with a small *PD-C* value in the downtown area and a large *PD-C* value at the urban fringes, indicating that the degree of fragmentation of artificially planted vegetation is low in the downtown area and high in the urban fringes.

4. Discussion

The long-term monitoring of urban dynamics is critical for understanding urbanization processes and their corresponding environmental consequences. Most studies have focused on monitoring urban expansion or landscape patterns, and only a few have explored the impact of urbanization on landscape patterns, especially urban green landscapes.^(29,34) In addition, vegetation is a vital component of the ecosystem and essential for human survival. Previous research has primarily focused on the spatiotemporal dynamics of urban expansion and landscape patterns, along with the qualitative analyses of the negative impacts of urbanization on these patterns. However, quantitative studies on how urbanization affects urban green landscape patterns, particularly artificial planting, are relatively scarce. Therefore, we developed a new framework to monitor the urban expansion dynamics and the impact of urbanization on urban green landscape patterns, especially the artificial planting of urban green landscapes in megacity Beijing using the time-series remote sensing imagery from 1999 to 2021.

The long-term monitoring of urban dynamics is conducive to further understanding the urbanization process, optimizing regional patterns, and promoting the sustainable development of the environment. Megacities are dynamic and complex systems, and monitoring and understanding their urban evolution process are necessary. However, few studies have explored monitoring urban expansion, particularly in megacities. In this study, we demonstrated that the urban area has been expanding from 1999 to 2021, the V_t and UEI of which were the largest from 2003 to 2009. This result agrees with that of a previous study,⁽²⁹⁾ which concluded that the total area of urban land increased exponentially by more than three times between 1985 and 2013 and that the largest increase in urban area occurred between 2005 and 2010. For a more accurate approach to extracting built-up areas, the *NTL* imagers are used instead of Landsat imagery. The NPP-VIIRS remote sensing images can reflect the frequency of human activities in a region and provide essential information for understanding and studying urban development. Visible light remote sensing data only represent the spatial extent of urbanization, while night light remote sensing data can reflect the internal changes of the city through pixel values.⁽²⁶⁾ Therefore, using night light remote sensing data to extract built-up areas plays an irreplaceable role in exploring the internal changes of built-up areas. The study of Li *et al.*⁽³⁵⁾ also proved that the urban extent extracted by the *SVM* method is overestimated in the suburbs, especially when only using Landsat images. The final map of the build-up area is illustrated in Fig. 17.

The spatial and temporal dynamics of urban growth in Beijing are compared in Fig. 17 using two different image sources (NPP-VIIRS/*NTL* and Landsat imagery). The build-up areas have expanded significantly from 1999 to 2021, particularly along the eastern and southern edges of the city. However, the Landsat images indicate a large extent of built-up areas compared with *NTL* data. The *NTL* data used in the proposed method can capture more detailed urban features, leading to a more accurate build-up area extraction.

Urban expansion significantly affects the original landscape pattern of a city, particularly its urban green landscape pattern. One class-level metric (*PD-C*) and three landscape-level metrics (*PD-L*, *ED*, and *SHDI*) were selected to quantify urban green landscape patterns, and the landscape presented spatial geometric heterogeneity in the urbanization process. With the

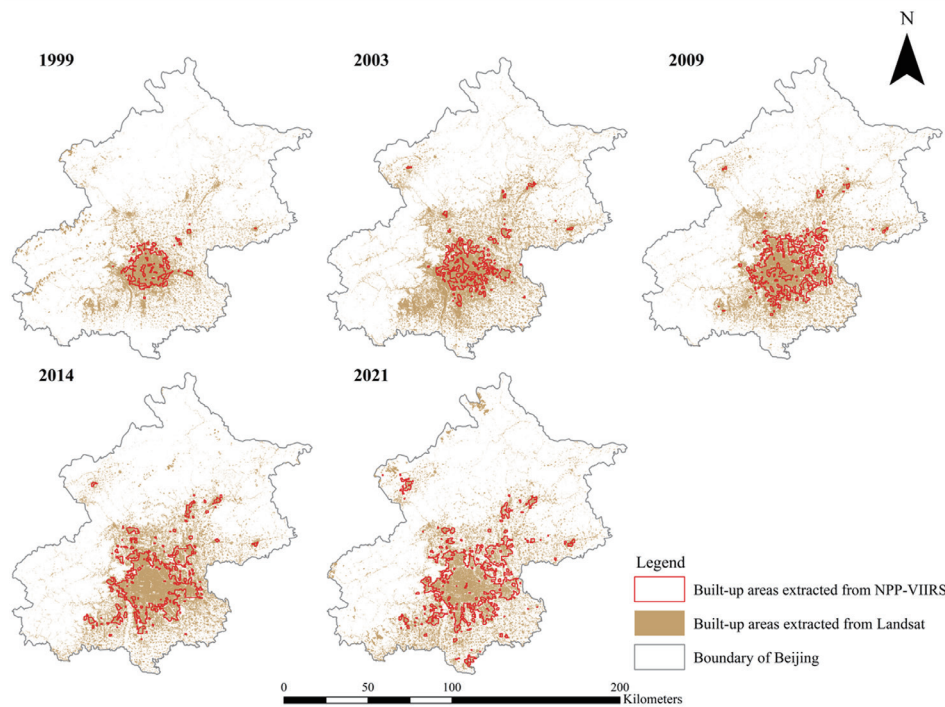


Fig. 17. (Color online) Map of build-up area extraction between NPP-VIIRS (*NTL*) and Landsat imagery.

acceleration of urbanization and the expansion of urban areas, the degree of landscape fragmentation has increased significantly in downtown and outer suburbs. This is similar to the results of Li *et al.*,⁽³⁶⁾ who concluded that the significant increase in *PD-L* in the downtown area was due to an increase in the degree of greening and that the increase in *PD-L* in the outer suburbs was mainly caused by the transformation from other land to construction land. Natural and seminatural vegetation gradually decreased in downtown areas along with the rapid expansion of the city from 1999 to 2009, and the diversity of the urban green landscape decreased, although some artificial green plants were planted. The diversity of urban green landscapes increased during the subsequent ten years, owing to the reasonable planning of urban green landscapes.

Studying the relationship between urbanization and urban green landscape patterns is an effective means of exploring the landscape ecological effects of urban expansion.⁽²⁰⁾ Therefore, the relationship between landscape patterns and NPP-VIIRS *NTL* value (*NLV*), which represents the level of urbanization, was explored in Fig. 18.

Figure 18 shows that there is a negative correlation between urban green landscape patterns and the level of urbanization, the *SHDI* of which at the landscape level and *NLV* had the greatest correlation, followed by *ED* and *PD-L*. The correlation coefficients between *PD-C* at the class level and *NLV* were the lowest, demonstrating that urban expansion has a negative effect on vegetation ecological landscape patterns. This conclusion is similar to Burak, Dog̃an, and Gaziog̃lu's findings,⁽³⁷⁾ which concluded that urban expansion has a certain degree of negative impact on the ecological environment. The higher the *NLV*, the higher the level of urbanization

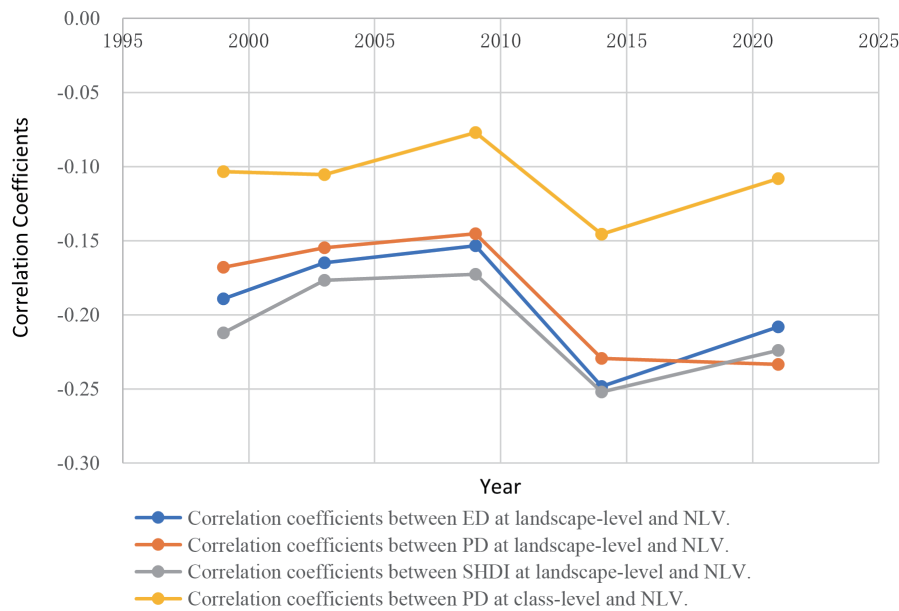


Fig. 18. (Color online) Correlation coefficients between landscape metrics and *NLV*.

construction, which leads to more fragmented urban green landscapes. This is in good agreement with the findings of Boori *et al.*,⁽³⁸⁾ who explored the relationship between urbanization and urban land use plans and concluded that vegetation patches became more fragmented owing to the increase in built-up area over the study period as a general trend at the metropolitan level. As the level of urbanization increased, the *SHDI* value decreased, indicating that urbanization negatively impacts regional habitat diversity. Zhang *et al.*⁽³⁹⁾ explored the characteristics of riparian plant diversity and its change law, and concluded that the more types of construction land there are, the greater the stress on biodiversity, especially the emergence of urban construction land, which leads to a significant decrease in biodiversity.

5. Conclusions

In this study, we quantified the spatiotemporal characteristics of urban expansion and urban green landscape patterns in Beijing using NPP-VIIRS *NTL* data and Landsat imagery from 1999 to 2021. The analysis revealed a significant outward expansion of the urban area, with the most rapid growth occurring between 2003 and 2009. This expansion has led to substantial alterations in landscape patterns, particularly impacting urban green landscapes.

The proposed approach demonstrated that the area of urban green landscapes decreased significantly owing to large-scale growth in built-up land. The degree of fragmentation of urban green landscapes was initially reduced from 1999 to 2009. Despite the ongoing expansion of built-up areas over the subsequent decade, efforts to construct new green spaces led to increases in the number of green patches and their degree of fragmentation. Furthermore, the diversity of urban green landscapes initially increased but later decreased, reflecting the ecological impacts of urban expansion.

This research provides valuable insights into how urbanization affects urban green landscape patterns, providing a theoretical basis and case reference for promoting sustainable landscape planning. By designing and optimizing landscape patterns, urban planners and policymakers can enhance the ecological benefits of urban landscapes, thereby promoting urban environments that are more sustainable in terms of resource use, resilience, and environmental balance. Although this study presents a comprehensive assessment framework, it faces certain limitations in the diversity and accuracy of data sources. The inability to fully leverage high-resolution remote sensing images (e.g., Sentinel-2 with 10 m resolution or WorldView-3 at 0.3 m) hinders the analysis of local dynamic changes. Moreover, the quantitative analysis of socioeconomic driving factors is insufficient. In the future, we will refine the analysis by integrating multisource, high-resolution remote sensing imagery with robust socioeconomic data. Furthermore, we will explore the driving mechanisms of urban expansion in greater depth and investigate the long-term impact of various expansion patterns on ecological service functions.

Acknowledgments

This work was supported by the R&D Program of Beijing Municipal Education Commission (No. KM202410016006), the Pyramid Talent Training Project for Beijing University of Civil Engineering and Architecture (No. JDYC20220824), the Fundamental Research Funds for Beijing University of Civil Engineering and Architecture (No. Y2207), and the National Natural Science Foundation of China (No. 42001379).

References

- 1 X. Li, Y. Zhou, J. Eom, S. Yu, and G. R. Asrar: *Earth's Future* **7** (2019) 351. <https://doi.org/10.1029/2019EF001152>
- 2 M. Zhao, Y. Zhou, X. Li, W. Cheng, C. Zhou, T. Ma, M. Li, and K. Huang: *Remote Sens. Environ.* **248** (2020) 111980. <https://doi.org/10.1016/j.rse.2020.111980>
- 3 Z. Zhu, Y. Zhou, K. C. Seto, E. C. Stokes, C. Deng, S. T. A. Pickett, and H. Taubenböck: *Remote Sens. Environ.* **228** (2019) 164. <https://doi.org/10.1016/j.rse.2019.04.020>
- 4 C. D. Elvidge, K. Baugh, M. Zhizhin, F. C. Hsu, and T. Ghosh: *Int. J. Remote Sens.* **38** (2017) 5860. <https://doi.org/10.1080/01431161.2017.1342050>
- 5 C. Yang, B. Yu, Z. Chen, W. Song, Y. Zhou, X. Li, and J. Wu: *Remote Sens.* **11** (2019) 2398. <https://doi.org/10.3390/rs11202398>
- 6 X. Li and Y. Zhou: *Int. J. Remote Sens.* **38** (2017) 6030. <https://doi.org/10.1080/01431161.2016.1274451>
- 7 Y. Yan, H. Lei, Y. Chen, and B. Zhou: *Remote Sens.* **14** (2022) 3212. <https://doi.org/10.3390/rs14133212>
- 8 Y. Zheng, Y. He, Q. Zhou, and H. Wang: *Sustainable Cities and Soc.* **76** (2022) 103338. <https://doi.org/10.1016/j.scs.2021.103338>
- 9 H. Dadashpoor, P. Azizi, and M. Moghadasi: *Sci. Total Environ.* **655** (2019) 707. <https://doi.org/10.1016/j.scitotenv.2018.11.267>
- 10 M. Zewdie, H. Worku, and A. Bantider: *Environ. Manage.* **61** (2018) 132. <https://doi.org/10.1007/s00267-017-0953-x>
- 11 M. Zhao, Y. Zhou, X. Li, W. Cao, C. He, B. Yu, X. Li, C. D. Elvidge, W. Cheng, and C. Zhou: *Remote Sens.* **11** (2019) 1971. <https://doi.org/10.3390/rs11171971>
- 12 C. He, P. Shi, J. Li, J. Chen, Y. Pan, J. Li, L. Zhuo, and Y. J. Ming: *Chin. Sci. Bull.* (2006) 856. <https://doi.org/10.3321/j.issn:0023-074X.2006.07.017>
- 13 P. Sutton: *Comput., Environ. Urban Syst.* **21** (1997) 227. [https://doi.org/10.1016/S0198-9715\(97\)01005-3](https://doi.org/10.1016/S0198-9715(97)01005-3)
- 14 W. T. Lawrence: *Remote Sens. Environ.* **61** (1997) 361. [https://doi.org/10.1016/S0034-4257\(97\)00046-1](https://doi.org/10.1016/S0034-4257(97)00046-1)
- 15 Y. Xie and Q. Weng: *Remote Sens. Environ.* **187** (2016) 1. <https://doi.org/10.1016/j.rse.2016.10.002>

- 16 C. Milesi, C. D. Elvidge, R. R. Nemani, and S. W. Running: *Remote Sens. Environ.* **86** (2003) 401. [https://doi.org/10.1016/S0034-4257\(03\)00081-6](https://doi.org/10.1016/S0034-4257(03)00081-6)
- 17 W. Jing, Y. Yang, X. Yue, and X. Zhao: *Remote Sens.* **7** (2015) 12419. <https://doi.org/10.3390/rs70912419>
- 18 C. He, Z. Liu, S. Gou, Q. Zhang, J. Zhang, and L. Xu: *Environ. Res. Lett.* **14** (2019) 034008. <https://doi.org/10.1088/1748-9326/aaf936>
- 19 J. Liu, W. Li, W. Zhou, L. Han, and Y. Qian: *Acta Ecologica Sinica* **38** (2018) 4341. <https://doi.org/10.5846/stxb201712312369>
- 20 X. Zhao and J. Liang: *J. Northwest University (Natural Science Edition)* **52** (2022) 391. <https://doi.org/10.16152/j.cnki.xdxbzr.2022-03-004>
- 21 S. Tagil, S. Gormus, and S. Cengiz: *J. Indian Soc. Remote Sensing* **46** (2018) 1285. <https://doi.org/10.1007/s12524-018-0801-3>
- 22 W. Su, C. Gu, G. Yang, S. Chen, and F. Zhen: *Landscape and Urban Plann.* **95** (2010) 61. <https://doi.org/10.1016/j.landurbplan.2009.12.003>
- 23 S. Karim, Y. Chen, P. M. Kayumba, I. Ahmad, and H. Iqbal: *J. Urban Manage.* (2024). <https://doi.org/10.1016/j.jum.2024.11.012>
- 24 K. Ben Messaoud, Y. Wang, P. Jiang, Z. Ma, K. Hou, and F. Dai: *Land* **13** (2024) 98. <https://doi.org/10.3390/land13010098>
- 25 Z. Chen, B. Yu, C. Yang, Y. Zhou, X. Qian, C. Wang, B. Wu, and J. Wu: *Earth Syst. Sci. Data Discuss.* **2020** (2020) 1. <https://doi.org/10.5194/essd-13-889-2021>
- 26 Q. Zheng, K. C. Seto, Y. Zhou, S. You, and Q. Weng: *ISPRS J. Photogramm. Remote Sens.* **202** (2023) 125. <https://doi.org/10.1016/j.isprsjprs.2023.05.028>
- 27 S. Kang, J. Choi, H. Yoon, and W. Choi: *Land Degrad. Dev.* **30** (2019) 2009. <https://doi.org/10.1002/ldr.3396>
- 28 J. Li and J. Pan: *J. Glaciol. Geocryology* **38** (2016) 829. <https://doi.org/10.7522/j.issn.1000-0240.2016.0093>
- 29 Y. Yang, Y. Liu, Y. Li, and G. Du: *Land Use Policy* **74** (2018) 220. <https://doi.org/10.1016/j.landusepol.2017.07.004>
- 30 T. P. s. G. o. B. Municipality: *The Master Plan of Beijing (2016–2035)*, <https://english.beijing.gov.cn/government/reports/> (September 24th, 2023)
- 31 T. P. s. G. o. B. Municipality: *Main Data of the 3rd National Land Resource Survey in Beijing City*, https://www.gov.cn/xinwen/2021-11/06/content_5649305.htm (September 23rd, 2023)
- 32 L. Chen, Q. Wei, Q. Fu, and D. Feng: *Land* **10** (2021) 167. <https://doi.org/10.3390/land10020167>
- 33 Q. Wang, S. Liu, Y. Liu, F. Wang, H. Liu, and L. Yu: *Global Ecol. Conserv.* **34** (2022) e02004. <https://doi.org/10.1016/j.gecco.2022.e02004>
- 34 D. Zhou, P. Shi, X. Wu, J. Ma, and J. Yu: *Sci. World J.* **2014** (2014) 821781. <https://doi.org/10.1155/2014/821781>
- 35 X. Li, L. Zhao, D. Li, and H. Xu: *Sensors* **18** (2018) 3665. <https://doi.org/10.3390/s18113665>
- 36 H. Li, J. Peng, L. Yanxu, and H. Yi'na: *Ecol. Indic.* **82** (2017) 50. <https://doi.org/10.1016/j.ecolind.2017.06.032>
- 37 S. Burak, E. Dog'an, and C. Gaziog'lu: *Ocean Coastal Manage.* **47** (2004) 515. <https://doi.org/10.1016/j.ocecoaman.2004.07.007>
- 38 M. S. Boori, M. Netzband, V. Vozenilek, and K. Choudhary: *Recent Adv. Electr. Eng.* **42** (2015) 99. <https://api.semanticscholar.org/CorpusID:42331643>
- 39 C. Zhang, C. Wang, R.-l. Sin, G.-f. Qie, H.-g. Bao, and S.-n. Tang: *J. Fujian Agriculture and Forestry University (Natural Science Edition)* **44** (2015) 520. [https://doi.org/10.13323/j.cnki.j.fafu\(nat.sci.\).2015.05.013](https://doi.org/10.13323/j.cnki.j.fafu(nat.sci.).2015.05.013)

About the Authors

Yanan Liu received her Ph.D. degree from Wuhan University, China, in 2020. Her research interest mainly focuses on remote sensing applications. Her specific research directions include high-resolution remote sensing image processing and analysis, key technologies and applications for forest analysis, and remote sensing. (liuyanana@bucea.edu.cn)

Mengxue Xu received her undergraduate degree from Beijing University of Civil Engineering and Architecture, China, in 2022. She is currently pursuing her M.S. degree in photogrammetry and remote sensing. Her research interest is in remote sensing applications. (2108160224004@stu.bucea.edu.cn)

Renjie Li is currently studying for his B.S. degree at Beijing University of Civil Engineering and Architecture, China. His research interest is in remote sensing applications.

(13618809863@163.com)

Ai Zhang received her undergraduate degree from Beijing University of Civil Engineering and Architecture, China, in 2023. She is currently pursuing her M.S. degree in photogrammetry and remote sensing. Her research interests are in remote sensing and forest analysis.

(2108570023082@stu.bucea.edu.cn)

Peng Gao received his B.S. degree from Beijing University of Civil Engineering and Architecture, China, in 2022, where he is currently pursuing his M.S. degree in photogrammetry and remote sensing. His research interests are in remote sensing and forest analysis.

(2108570022088@stu.bucea.edu.cn)